Hindawi
Shock and Vibration
Volume 2019, Article ID 3476826, 12 pages
https://doi.org/10.1155/2019/3476826

Research Article

Smith Predictor-Taylor Series-Based LQG Control for Time Delay Compensation of Vehicle Semiactive Suspension

Laihua Tao,[1] **Shian Chen**,[1] **Guisheng Fang**,[1] **and Guanghao Zu**[2]

[1]*School of Mechanical and Automotive Engineering, Zhejiang University of Water Resources and Electric Power, Hangzhou 310018, China*
[2]*Department of Automotive Engineering, Suqian Zeda Vocational & Technical College, Suqian 223800, China*

Correspondence should be addressed to Laihua Tao; 995778970@qq.com

Received 26 March 2019; Revised 13 May 2019; Accepted 25 May 2019; Published 12 June 2019

Academic Editor: Mario Terzo

A Smith predictor-Taylor series-based LQG (STLQG) control to compensate time delay of a semiactive suspension system is newly presented. This control consists of a Taylor series-based LQG (TLQG) control and a Smith predictor based on the TLQG. The TLQG control compensates one half of time delay to decrease magnification from whole time delay compensation. The Smith predictor based on the TLQG compensates the other half to decrease horizontal shift from whole time delay compensation using the Smith predictor-based LQG. Finally, a practical case illustrates advantages of the STLQG control.

1. Introduction

Recently, research studies on vehicle vibration suppression using semiactive suspensions have significantly increased [1–4]. In a semiactive suspension system, time delay is usually inevitable because of the time spent in measuring system state, calculating and generating controls, etc [5–7]. The response process of magnetorheological semiactive suspension includes suspension system perceiving excitation, obtaining excitation information, control unit computing and sending out control information, and suspension generating controllable damping force to realize system vibration reduction. If the response time of some links is too long, the system response time delay will occur. Actuators of semiactive suspensions include magnetorheological damper, electrorheological damper, variable orifice damper, and so on [8, 9]. Among those semiactuators, magnetorheological damper is well known as having the fastest response [10–13]. Magnetorheological semiactive suspension is considered in this work. References [14, 15] reported that time delay of a magnetorheological semiactive suspension system was about 25 ms. Time delay generally has a great impact on the semiactive suspension system and makes a satisfactory controller difficult to be designed. When time delay is not taken into account, it may badly degrade performance and even lead to instability [16–20]. So, this article discusses the system under 15 ms, 20 ms, 25 ms, and 30 ms time delay.

A common compensation strategy for time delay is the application of Smith predictor in control systems [21–23]. Zhao et al. used fuzzy control strategy and Smith predictor to compensate time delay for a time-delayed suspension, and simulation was carried out by Matlab/Simulink. The simulation result showed that the time delay-compensated system could improve the performance of the semiactive suspension. In his simulation model, a time delay loop was set on output line of state vector, i.e., sensors. However, the semiactive suspension's time delay was mainly caused by its actuator. So, the time delay loop should be put on the actuator [15]. Yu et al. presented a control strategy using LQG and Smith predictor to compensate time delay in a semiactive suspension system. His research showed that the effect of time delay on unsprung mass vibration was larger than that on sprung mass vibration. But basal damping was relatively large in his simulation model, which had a great influence on the time-delayed system. What's more, weights of LQG

control for the suspension were not given [24]. But, when time delay was rather large, the Smith-LQG (SLQG) control's effect was unsatisfactory because the control force from the SLQG control had a larger horizontal shift compared with the ideal control force. Furthermore, its performance is worse than a passive suspension system when time delay is larger than 30 ms.

Song and Xu investigated stochastic preview control with time delay consideration for an active vehicle suspension system with a look-ahead sensor. Design of the preview compensator was reduced to the classical LQG control problem, by converting the state equations and the performance index into discrete forms and augmenting the state and output vectors. In their research, though LQG control was utilized, the quadratic performance index comparison was not provided [25].

This paper aims at developing a new Smith predictor-Taylor series-based LQG (STLQG) control to improve the performance of a time-delayed semiactive suspension system. The idea of combining LQG and Taylor series to compensate time delay is proposed, and a practical Taylor series-based LQG (TLQG) control is developed. In the STLQG control, time delay compensation is divided into two parts. The TLQG control compensates one half time delay and is based on which the Smith predictor based on the TLQG is designed to further compensate the other half time delay. In this way, the amplification of the TLQG control is weakened and the horizontal shift of the SLQG control force is reduced.

The remainder of this work is arranged as follows: first, the TLQG control is proposed for a time-delayed semiactive suspension in Section 2, and we settle the difficulty of directly combining LQG with the Taylor series. In Section 3, an STLQG controller is designed. A practical case is given to show the effectiveness of the STLQG control for time delay compensation in Section 4. Finally, the conclusion comes in Section 5.

2. TLQG Control for Semiactive Suspension

In this section, we consider a quarter-vehicle semiactive suspension system with time delay as depicted in Figure 1.

The differential equations of motion considering time delay can be written as follows:

$$\begin{cases} m_1\ddot{z}_1 + c_s(\dot{z}_1 - \dot{z}_2) + k_1(z_1 - q) + k_2(z_1 - z_2) = -F_{sa}, \\ m_2\ddot{z}_2 + c_s(\dot{z}_2 - \dot{z}_1) + k_2(z_2 - z_1) = F_{sa}, \end{cases} \tag{1}$$

where m_1 and m_2 are the unsprung and sprung masses, respectively; k_1 and k_2 are the tire and suspension stiffnesses, respectively; z_1 and z_2 are the vertical displacements of the unsprung and sprung masses, respectively; c_s is the basal damping; F_{sa} is actual semiactive control force; and q is the displacement input of the suspension system from the road irregularity, which is expressed as

$$\dot{q} = -2\pi f_0 q + 2\pi n_0 w\sqrt{G_q(n_0)v}, \tag{2}$$

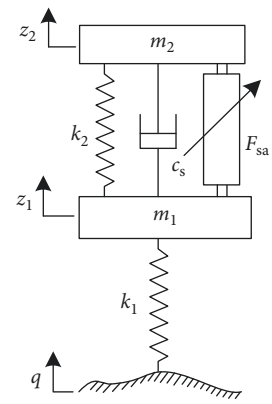

Figure 1: Quarter-vehicle model.

where n_0 is the reference spatial frequency and equals 0.1; w is the white noise signal of the road; $G_q(n_0)$ is the road irregularity coefficient under n_0 determined by the road class; v is the vehicle speed; and f_0 is the lower cut off frequency and equals $0.011v$.

The system state vector is chosen as

$$\begin{aligned} \mathbf{X} &= (x_1, x_2, x_3, x_4)^T, \\ x_1 &= z_1 - q, \\ x_2 &= z_2 - z_1, \\ x_3 &= \dot{z}_1, \\ x_4 &= \dot{z}_2. \end{aligned} \tag{3}$$

The state equation of the time-delayed semiactive suspension system is expressed as follows:

$$\dot{\mathbf{X}} = \mathbf{AX} + \mathbf{BU} + \mathbf{GW}, \tag{4}$$

where

$$\mathbf{A} = \begin{bmatrix} 0 & 0 & 1 & 0 \\ 0 & 0 & -1 & 1 \\ -\dfrac{k_1}{m_1} & \dfrac{k_2}{m_1} & -\dfrac{c_s}{m_1} & \dfrac{c_s}{m_1} \\ 0 & -\dfrac{k_2}{m_2} & \dfrac{c_s}{m_2} & -\dfrac{c_s}{m_2} \end{bmatrix}, \tag{5}$$

$$\mathbf{B} = \begin{bmatrix} 0 & 0 & -\dfrac{1}{m_1} & \dfrac{1}{m_2} \end{bmatrix}^T,$$

$$\mathbf{G} = \begin{bmatrix} -1 & 0 & 0 & 0 \end{bmatrix}^T,$$

$$\mathbf{U} = [F_{sa}],$$

$$\mathbf{W} = [w].$$

2.1. Idea and Practical Method of LQG Based on Taylor Series for Time-Delay Compensation. Here, we take all the time spent in measuring the system state and calculating and generating the active actual control F_{aa} as an integral time delay loop. When LQG control is used and there is not any time delay compensation countermeasure, F_{aa} is written as

$$F_{aa} = F_i(t-\tau), \tag{6}$$

where, F_i is the idea control; τ is time delay.

To improve control effect, we propose to use the first-order Taylor series to predict control force F_p ahead to compensate time delay as follows:

$$F_p = F_i(t+\tau) \approx F_i + \tau \dot{F}_i. \tag{7}$$

After the above compensation measure is adopted, equation (5) is expressed as

$$F_{aa} = F_p(t-\tau) = F_i. \tag{8}$$

Here, to compensate time delay, we replace F_i by and F_{aa} and solve F_{aa} during the new LQG controller design.

Combing and rearranging equations (4) and (7) gives

$$\begin{aligned} \dot{\mathbf{X}}_1 &= \mathbf{A}_0\mathbf{X}_1 + \mathbf{B}_0\mathbf{U}_0 + \mathbf{G}_0\mathbf{W}, \\ \mathbf{X}_1 &= \left[\mathbf{X}^T, F_i\right]^T, \\ \mathbf{U}_0 &= \left[F_p\right], \end{aligned} \tag{9}$$

where

$$\mathbf{A}_0 = \begin{bmatrix} 0 & 0 & 1 & 0 & 0 \\ 0 & 0 & -1 & 1 & 0 \\ -\frac{k_1}{m_1} & \frac{k_2}{m_1} & -\frac{c_s}{m_1} & \frac{c_s}{m_1} & -\frac{1}{m_1} \\ 0 & -\frac{k_2}{m_2} & \frac{c_s}{m_2} & -\frac{c_s}{m_2} & \frac{1}{m_2} \\ 0 & 0 & 0 & 0 & -\frac{1}{\tau} \end{bmatrix}, \tag{10}$$

$$\mathbf{G}_0 = \begin{bmatrix} -1 & 0 & 0 & 0 & 0 \end{bmatrix}^T,$$

$$\mathbf{B}_0 = \begin{bmatrix} 0 & 0 & 0 & 0 & \frac{1}{\tau} \end{bmatrix}^T.$$

During designing the LQG controller for equation (9), the suspension quadratic performance index J is expressed as follows [26]:

$$\begin{aligned} J &= \lim_{T\to\infty} \frac{1}{T} \int_0^T \left[\ddot{z}_2^2 + \delta_1 (z_1 - q)^2 + \delta_2 (z_2 - z_1)^2\right] dt \\ &= \lim_{T\to\infty} \frac{1}{T} \int_0^T \left[\mathbf{X}_1^T \mathbf{Q}_0 \mathbf{X}_1 + 2\mathbf{X}_1^T \mathbf{N}_0 \mathbf{U}_0 + \mathbf{U}_0^T \mathbf{R}_0 \mathbf{U}_0\right] dt, \end{aligned}$$

$$\mathbf{Q}_0 = \begin{bmatrix} \delta_1 & 0 & 0 & 0 & 0 \\ 0 & \delta_2 + \frac{k_2^2}{m_2^2} & -\frac{k_2 c_s}{m_2^2} & \frac{k_2 c_s}{m_2^2} & -\frac{k_2}{m_2^2} \\ 0 & -\frac{k_2 c_s}{m_2^2} & \frac{c_s^2}{m_2^2} & -\frac{c_s^2}{m_2^2} & \frac{c_s}{m_2^2} \\ 0 & \frac{k_2 c_s}{m_2^2} & -\frac{c_s^2}{m_2^2} & \frac{c_s^2}{m_2^2} & -\frac{c_s}{m_2^2} \\ 0 & -\frac{k_2}{m_2^2} & \frac{c_s}{m_2^2} & -\frac{c_s}{m_2^2} & \frac{1}{m_2^2} \end{bmatrix},$$

$$\mathbf{N}_0 = \begin{bmatrix} 0 & 0 & 0 & 0 & 0 \end{bmatrix}^T,$$

$$\mathbf{R}_0 = [0], \tag{11}$$

where $\ddot{z}_2$ is the sprung mass acceleration; $(z_1 - q)$ is the tire deflection and is equal to the tire dynamic load divided by k_1; $(z_2 - z_1)$ is the suspension deflection; δ_1 and δ_2 are the weights of $(z_1 - q)^2$ and $(z_2 - z_1)^2$, respectively, when the weight of $\ddot{z}_2^2$ is set as 1; T is the total duration at which the vehicle runs; and t is the time variable. The smaller J is, the better the suspension performance is, when J is used to evaluate ride comfort.

According to reference [27], when the following conditions are true, the LQG controller for equation (9) can be designed:

(i) The pair $(\mathbf{A}_0, \mathbf{B}_0)$ is stabilizable;

(ii) $\mathbf{R}_0 > \mathbf{0}$ and $\mathbf{Q}_0 - \mathbf{N}_0 \mathbf{R}_0^{-1} \mathbf{N}_0^T \geq 0$.

Checking equations (9) and (11), we can find that (i) is true and $\mathbf{Q}_0 - \mathbf{N}_0 \mathbf{R}_0^{-1} \mathbf{N}_0^T \geq 0$, but (ii) is not satisfied because $\mathbf{R}_0$ equals 0. So, there should be necessary modification on equation (9) to make the LQG control based Taylor series compensating time delay work smoothly.

2.2. TLQG Controller Design. To ensure that the condition $\mathbf{R}_0 > 0$ is true, a novel transformation on F_p is presented as follows:

$$\begin{cases} F_p \approx F_i(t+\tau) \approx F_i + \tau \dot{F}_i, \\ \beta + b = 1, \quad \beta \gg b, \\ F_i \longleftarrow \beta F_i + b F_p. \end{cases} \tag{12}$$

Considering the tire stiffness is almost 9 times larger than the suspension stiffness, so the vertical displacement of the unsprung mass under normal operating frequency range can be taken as the road input. Through this kind of approximation method, the vertical displacement of the unsprung mass measurement can be directly used as the input of the extended function [28].

The new extended function and J are written as follows:

$$\dot{\mathbf{X}}_1 = \mathbf{A}_1\mathbf{X}_1 + \mathbf{B}_1\mathbf{U}_1 + \mathbf{G}_1\mathbf{W}_1, \tag{13}$$

$$J = \frac{1}{T}\int_0^T \left[\mathbf{X}_1^T\mathbf{Q}_1\mathbf{X}_1 + 2\mathbf{X}_1^T\mathbf{N}_1\mathbf{U}_1 + \mathbf{U}_1^T\mathbf{R}_1\mathbf{U}_1\right]dt, \tag{14}$$

where

$$\mathbf{U}_1 = \mathbf{U}_0,$$

$$\mathbf{W}_1 = [z_1],$$

$$\mathbf{G}_1 = \mathbf{G}_0,$$

$$\mathbf{A}_1 = \begin{bmatrix} 0 & 0 & 1 & 0 & 0 \\ 0 & 0 & -1 & 1 & 0 \\ -\frac{k_1}{m_1} & \frac{k_1}{m_1} & -\frac{c_s}{m_1} & \frac{c_s}{m_1} & -\frac{\beta}{m_1} \\ 0 & -\frac{k_2}{m_2} & \frac{c_s}{m_2} & -\frac{c_s}{m_2} & \frac{\beta}{m_2} \\ 0 & 0 & 0 & 0 & -\frac{1}{\tau} \end{bmatrix},$$

$$\mathbf{B}_1 = \begin{bmatrix} 0 & 0 & -\frac{b}{m_1} & \frac{b}{m_2} & \frac{1}{\tau} \end{bmatrix}^T, \tag{15}$$

$$\mathbf{Q}_1 = \begin{bmatrix} \delta_1 & 0 & 0 & 0 & 0 \\ 0 & \delta_2 + \frac{k_2^2}{m_2^2} & -\frac{k_2c_s}{m_2^2} & \frac{k_2c_s}{m_2^2} & -\frac{\beta k_2}{m_2^2} \\ 0 & -\frac{k_2c_s}{m_2^2} & \frac{c_s^2}{m_2^2} & -\frac{c_s^2}{m_2^2} & \frac{\beta c_s}{m_2^2} \\ 0 & \frac{k_2c_s}{m_2^2} & -\frac{c_s^2}{m_2^2} & \frac{c_s^2}{m_2^2} & -\frac{\beta c_s}{m_2^2} \\ 0 & -\frac{\beta k_2}{m_2^2} & \frac{\beta c_s}{m_2^2} & -\frac{\beta c_s}{m_2^2} & \frac{\beta^2}{m_2^2} \end{bmatrix},$$

$$\mathbf{N}_1 = \begin{bmatrix} 0 & -\frac{bk_2}{m_2^2} & \frac{bc_s}{m_2^2} & -\frac{bc_s}{m_2^2} & \frac{\beta b}{m_2^2} \end{bmatrix}^T,$$

$$\mathbf{R}_1 = b^2\mathbf{R}.$$

After the above transformation, the control system described by equation (13) is almost equal to the one described by equation (4) because $\beta \gg b$.

In this time, $\mathbf{R}_1 > 0$, and those newly obtained matrixes in equations (13) and (14) satisfy the work requirements of the LQR function.

The block diagram of the LQG controller for equation (13) is shown in Figure 2, and the design process is explained in the following sections.

The optimal feedback gain matrix $\mathbf{K}_1$ of the TLQG controller is obtained as follows:

$$(\mathbf{K}_1, \mathbf{S}_1, \mathbf{E}_1) = \mathrm{LQR}(\mathbf{A}_1, \mathbf{B}_1, \mathbf{Q}_1, \mathbf{N}_1, \mathbf{R}_1). \tag{16}$$

We obtain

$$F_p = -\mathbf{K}_1\mathbf{X}_1. \tag{17}$$

The actual semiactive control force is obtained as follows:

$$F_{sa} = \begin{cases} F_p(t-\tau), & \text{when } (\dot{z}_2 - \dot{z}_1)F_p < 0, \\ 0, & \text{else.} \end{cases} \tag{18}$$

Checking equations (5)–(8), we find that F_{aa} nearly equals F_i when τ is very small, and F_p will be magnified too much when time delay is rather large. This amplification will weaken the control effect.

To solve the amplification problem, the STLQG control is presented.

3. STLQG Control for Semiactive Suspension

The principle and block diagram of the STLQG controller for compensating time delay of the semiactive suspension is presented in Figures 3 and 4, respectively.

As shown in Figures 3 and 4, the STLQG controller consists of two controllers: the first controller comprised by the extended function and the Taylor-LQG control and the second controller composed of Smith predictor and the Taylor-LQG control.

The piecewise compensation is used in this control: The first controller compensates one half of time delay to decrease magnification from whole time delay compensation and the second controller compensates the other half to decrease horizontal shift from whole time delay compensation using the Smith predictor based on the LQG.

Specifically, the output of the extended function is the ideal active control force F_i which will be combined with the state vector of the plant to predict $F_{p1} \approx F_i(t + (\tau/2))$ using the first-order Taylor series. On the basis of F_{p1}, the second controller calculates F_{p2} to improve the TLQG's ability to track F_i. F_{p1} and F_{p2} contribute the predicted force $F_{p3} \approx F_i(t + \tau)$ which is the final predicted active control force.

The actual control force F_{sa} is generated by the time-delayed semiactive control force actuator as follows:

$$F_{sa} = \begin{cases} F_{p3}(t-\tau), & \text{when } (\dot{z}_2 - \dot{z}_1)F_{p3} < 0, \\ 0, & \text{else.} \end{cases} \tag{19}$$

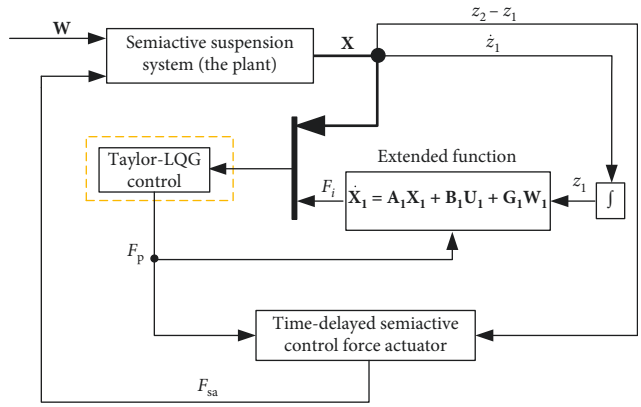

Figure 2: Block diagram of the TLQG controller.

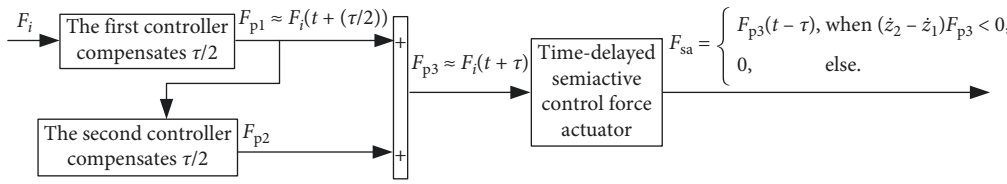

Figure 3: Principle of the STLQG control system.

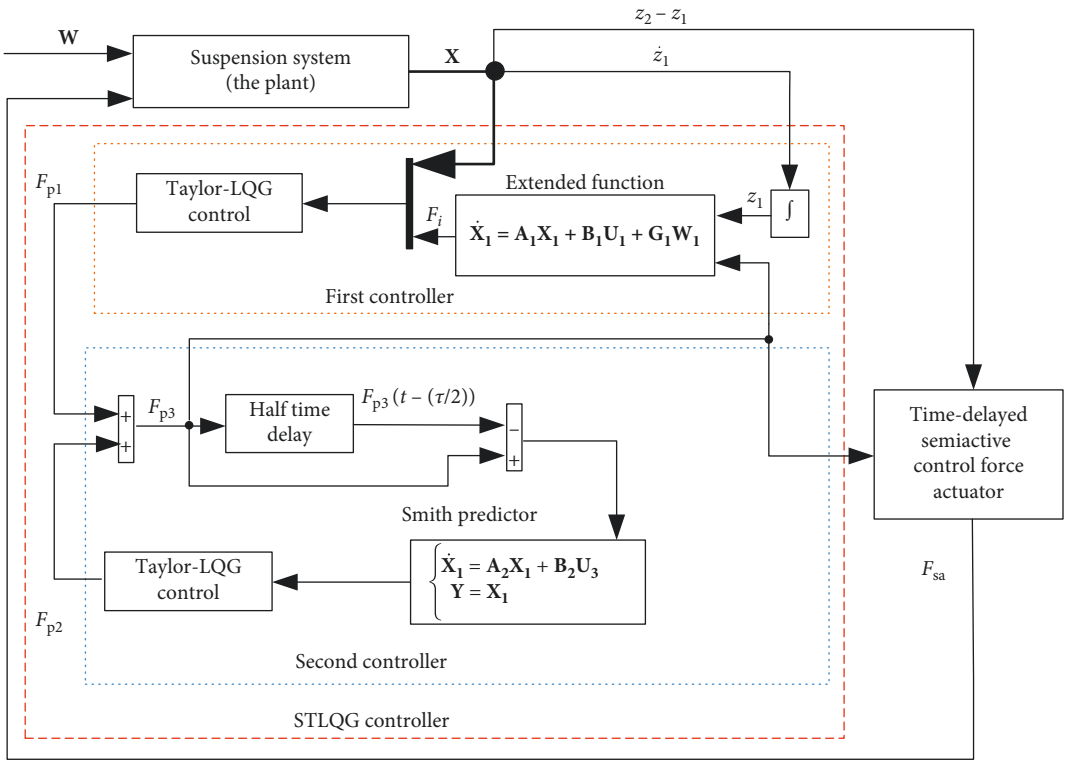

Figure 4: Block diagram of STLQG control system.

3.1. First Controller's Design. According to the TLQG controller design and the piecewise compensation, τ should be replaced by $\tau/2$ in the first controller.

$$\begin{cases} F_{\mathrm{p1}} = F_i\left(t+\dfrac{\tau}{2}\right) \approx F_i + \dfrac{\tau}{2}\dot{F}_i, \\ \beta + b = 1, \quad \beta \gg b, \\ F_i \longleftarrow \beta F_i + bF_{\mathrm{p1}}. \end{cases} \tag{20}$$

After combining equation (20) with equation (4), the extended function can be obtained:

$$\dot{\mathbf{X}}_1 = \mathbf{A}_2\mathbf{X}_1 + \mathbf{B}_2\mathbf{U}_2 + \mathbf{G}_2\mathbf{W}_2, \tag{21}$$

where

$$\mathbf{U}_2 = \left[F_{p1}\right],$$

$$\mathbf{A}_2 = \begin{bmatrix} 0 & 0 & 1 & 0 & 0 \\ 0 & 0 & -1 & 1 & 0 \\ -\dfrac{k_1}{m_1} & \dfrac{k_1}{m_1} & -\dfrac{c_s}{m_1} & \dfrac{c_s}{m_1} & -\dfrac{\beta}{m_1} \\ 0 & -\dfrac{k_2}{m_2} & \dfrac{c_s}{m_2} & -\dfrac{c_s}{m_2} & \dfrac{\beta}{m_2} \\ 0 & 0 & 0 & 0 & -\dfrac{2}{\tau} \end{bmatrix}, \tag{22}$$

$$\mathbf{B}_2 = \begin{bmatrix} 0 & 0 & -\dfrac{b}{m_1} & \dfrac{b}{m_2} & \dfrac{2}{\tau} \end{bmatrix}^T,$$

$$\mathbf{G}_2 = \mathbf{G}_1,$$

$$\mathbf{W}_2 = \mathbf{W}_1.$$

J is rewritten as follows:

$$J = \frac{1}{T}\int_0^T \left[\mathbf{X}_1^T\mathbf{Q}_2\mathbf{X}_1 + 2\mathbf{X}_1^T\mathbf{N}_2\mathbf{U}_2 + \mathbf{U}_2^T\mathbf{R}_2\mathbf{U}_2\right]dt, \tag{23}$$

where

$$\begin{aligned} \mathbf{Q}_2 &= \mathbf{Q}_1, \\ \mathbf{N}_2 &= \mathbf{N}_1, \\ \mathbf{R}_2 &= \mathbf{R}_1. \end{aligned} \tag{24}$$

The optimal feedback gain matrix $\mathbf{K}_2$ of the TLQG controller is obtained as follows:

$$\left(\mathbf{K}_2, \mathbf{S}, \mathbf{E}\right) = \mathrm{LQR}\left(\mathbf{A}_2, \mathbf{B}_2, \mathbf{Q}_2, \mathbf{N}_2, \mathbf{R}_2\right). \tag{25}$$

We obtain

$$F_{\mathrm{p1}} = -\mathbf{K}_2\mathbf{X}_1. \tag{26}$$

3.2. Second Controller's Design. According to Smith predictor design method and the extended function, the Smith predictor based on the TLQG control is designed as follows [29, 30].

Assume that the system described by equation (4) had no time delay, so its transfer function is

$$\begin{aligned} \frac{y(s)}{w(s)} &= \left[\mathbf{I} + \mathbf{H}(s)\mathbf{G}(s)\right]^{-1}\mathbf{H}_G(s), \\ \mathbf{H}_G(s) &= (s\mathbf{I} - \mathbf{A})^{-1}\mathbf{G}(s). \end{aligned} \tag{27}$$

Actually, there must be time delay in the system depicted by equation (4). The transfer function for the time-delayed semiactive suspension system with the Smith predictor is

$$\frac{y(s)}{w(s)} = \left[\mathbf{I} + \mathbf{H}(s)\mathbf{G}(s)\right]^{-1}\left[\mathbf{I} + \mathbf{H}(s)\mathbf{G}(s) - \mathbf{H}(s)\mathbf{G}(s)e^{-\tau s}\right]\mathbf{H}_G(s). \tag{28}$$

When $\tau = 0$, the transfer function in equation (27) is the same as that in equation (28). Further, the magnitude of equation (27) is quite close to that of equation (28) when the time delay τ is very small. However, as τ increases, the magnitude of equation (28) will differ significantly from that of equation (27) and the performance of Smith predictor will degrade.

In the proposed STLQG control strategy, the Smith predictor implemented in time-domain is given as follows [31]:

$$\begin{cases} \dot{\mathbf{X}}_1 = \mathbf{A}_2\mathbf{X}_1 + \mathbf{B}_2\mathbf{U}_3, \\ \mathbf{Y} = \mathbf{X}_1, \\ \mathbf{U}_3 = \left[F_{\mathrm{p3}} - F_{\mathrm{p3}}\left(t-\dfrac{\tau}{2}\right)\right]. \end{cases} \tag{29}$$

The Smith predictor has no disturbance input and the compensation of F_1 can be obtained by its output and LQG controller, i.e., $F_{\mathrm{p2}} = -\mathbf{K}_2\mathbf{X}_1$. Then the predicted force $F_{\mathrm{p3}} = F_{\mathrm{p1}} + F_{\mathrm{p2}}$ is figured out.

According to regulation shown by equation (18), the time-delayed semiactive force actuator turns F_{p3} into the actual control force of the plant.

4. Simulation Study and Results

In order to explain the advantages of the proposed method, several types of simulation comparisons are made: performance comparisons among the passive suspension (suspension with constant damping and stiffness parameters) and LQG, SLQG, TLQG, and STLQG control semiactive suspension.

The vehicle parameters studied in this research are listed in Table 1.

c_0 is the passive damping value of the passive suspension. The nominal running condition is assumed to be the vehicle running on a C-class road whose road irregularity coefficient is $256\times10^{-6}\,\mathrm{m}^2/\mathrm{m}^{-1}$ at the speed of 20 m/s.

Table 1: Parameters needed in this research.

Parameter	Value
m_1 (kg)	35
m_2 (kg)	500
k_1 (N/m)	300000
k_2 (N/m)	50500
c_0 (Ns/m)	3015
c_s	600
B	0.999
B	0.001

According to the method of deciding weights in reference for LQG control [32], we can obtain $\delta_1 = 53775$ and $\delta_2 = 4108.8$. In a magnetorheological semiactive suspension system, time delay is about 25 ms. Therefore, we discuss the system under 15 ms, 20 ms, 25 ms, and 30 ms time delay.

In the following figures and table, Passive stands for the passive suspension, LQG stands for the common LQG control (without time delay compensation), TLQG means the TLQG control, SLQG stands for the SLQG control, and STLQG stands for the STLQG control.

4.1. Actual Semiactive Control Force Comparisons among the SLQG, TLQG, and STLQG Controls and Their Corresponding Ideal LQG Controls (without Time Delay). With time delay increasing, the actual semiactive control force deteriorates and gradually loses the ability to track their corresponding ideal semiactive control force, which worsens the overall performance of the time-delayed system. Therefore, the actual semiactivecontrol force comparisons are discussed.

The F_a-t curve comparisons among the STLQG, SLQG, and TLQG controls and their corresponding ideal LQG controls under 15 ms, 20 ms, 25 ms, and 30 ms time delay are illustrated in Figures 5–8. F_a means the actual semiactive control force. SLQG$_i$ stands for the ideal LQG control which calculates the ideal semiactive control force using the state vector of the SLQG control system. TLQG$_i$ represents the ideal LQG control which obtains the ideal semiactive control force using the state vector of the TLQG control system. Similarly, STLQG$_i$ means the ideal LQG control that calculates the ideal semiactive control force utilizing the STLQG control system's state vector. The closer the F_a-t curve to the ideal semiactive control curve, the better the time delay compensation effect should be.

As shown in Figures 5–8, the F_a-t curve of the TLQG control is in relatively large disparity with that of the TLQG$_i$ control. Furthermore, the fluctuation trend of the TLQG control force is similar to the TLQG$_i$ semiactive control force and the disparity mainly displays in the amplitude of F_a. It is because if τ is rather large, F_1 will be magnified too much so that there is a serious discrepancy between the TLQG control force and the ideal control input. This phenomenon will worsen the performance of the TLQG controller. Horizontal shift of the TLQG control, however, is minor.

For the SLQG control, it has relatively minor amplitude discrepancies with the ideal semiactive control force. Furthermore, the amplitude of the SLQG semiactive control force is closer to that of the SLQG$_i$ control, compared with the TLQG control. However, the horizontal shift of the SLQG F_a-t curve is larger than that of the TLQG F_a-t curve.

It can be observed from Figures 5–8 that the STLQG controller has the strongest ability to track the ideal control. This suggests that the amplification problem of Taylor series is weaken by the piecewise compensation and the SLQG control. What's more, the STLQG control force has smaller horizontal shift than the SLQG control force, i.e., the advantage of the TLQG control has been used.

To further compare the actual semiactive control, simulation results of the actual semiactive control force are listed in Table 2. F_d represents the difference between the actual semiactive control force and the ideal semiactive control force. σ (F_d) stands for the mean square error of F_d. The smaller σ (F_d) is, the better the ability to track the ideal semiactive control force is.

As shown in Table 2, σ (F_d) of the STLQG control is less than that of the SLQG and TLQG control as time is 20 ms, 25 ms, and 30 ms, which means the STLQG control has stronger ability to track the ideal semiactive control force. σ (F_d) of the TLQG control is the smallest among the three as time delay is 15 ms; however, it will be more than that of the SLQG and STLQG control when time delay increases.

4.2. Performance Comparisons among the LQG, SLQG, TLQG, and STLQG Controls. Figures 9–12 exhibit the J-t curves utilizing the Passive, SLQG, TLQG, LQG, and STLQG controllers as time delay is 15 ms, 20 ms, 25 ms, and 30 ms, respectively.

It can be observed from Figures 9–12 that the TLQG control is relatively superior to the SLQG and STLQG controls when time delay is small. The control effect of the Passive, SLQG, and TLQG controls, however, will grow closer with time delay increasing. For the LQG control, it is better than the Passive control when time delay is 15 ms and 20 ms. But the LQG control is clearly worse than the Passive control while time delay increases to 25 ms. Hence, the curves of the LQG controller are not shown in Figures 12–16. The STLQG control has a more significant advantage than the SLQG, TLQG, Passive, and LQG controls.

The PSD (a_2)-frequency curve comparisons among the Passive, SLQG, TLQG, and STLQG controls under 15 ms, 20 ms, 25 ms, and 30 ms time delay are illustrated in Figures 13–16. a_2 represents the acceleration of the sprung mass and is also an important performance evaluator. The smaller the deviation of PSD (a_2) is, the more comfortable the ride is.

As shown in Figures 13–16, ride comfort deteriorates with the increase of time delay. The STLQG controller is effective in reducing the peak of PSD (a_2), and it always has better ride comfort than the Passive control. For the SLQG control, its PSD (a_2)-Frequency curve has a higher peak than

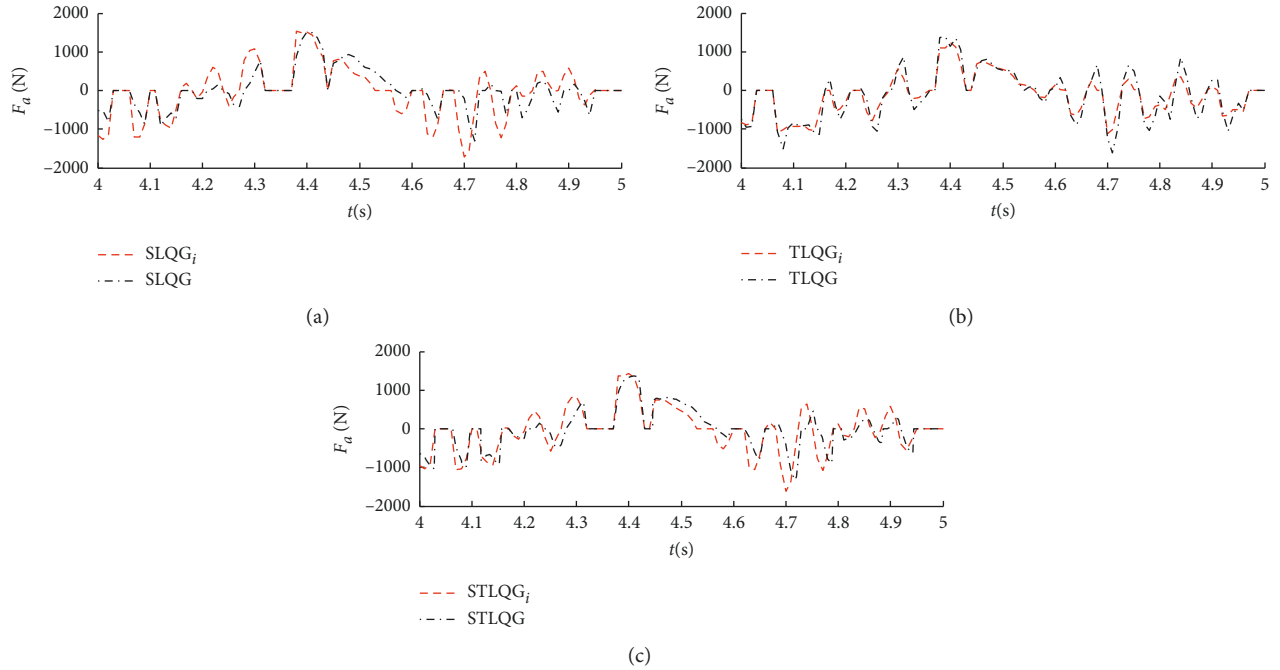

Figure 5: F_a-t curves under 15 ms time delay (partial enlargement).

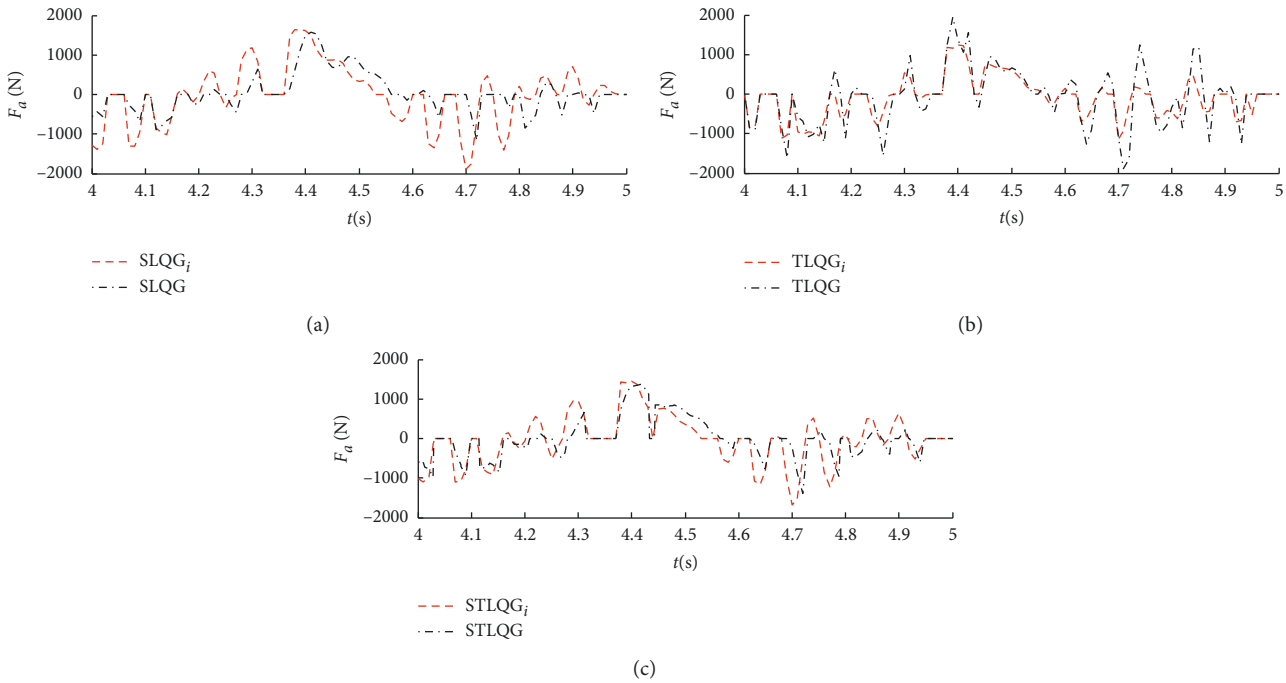

Figure 6: F_a-t curves under 20 ms time delay (partial enlargement).

the Passive control as the frequency is about 2 Hz. The TLQG control has relatively better ride comfort than the Passive control, but its ride comfort is worse than the Passive control when frequency is between 17 Hz and 22 Hz. STLQG slightly sacrifices the low-frequency performance, so that the high-frequency performance is greatly improved, On the whole, the STLQG control has more excellent ride comfort than the Passive, SLQG, and TLQG controls.

J-t curves demonstrate the overall performance of the controllers. However, J weighs the acceleration of the sprung mass, the tire deflection, and the suspension deflection. As it is well known, all the three elements have a great influence on the suspension performance so that due attention should be attached to them. In order to further illustrate the comparisons, the root-mean-square value of the three elements and J are listed in Table 3. In the

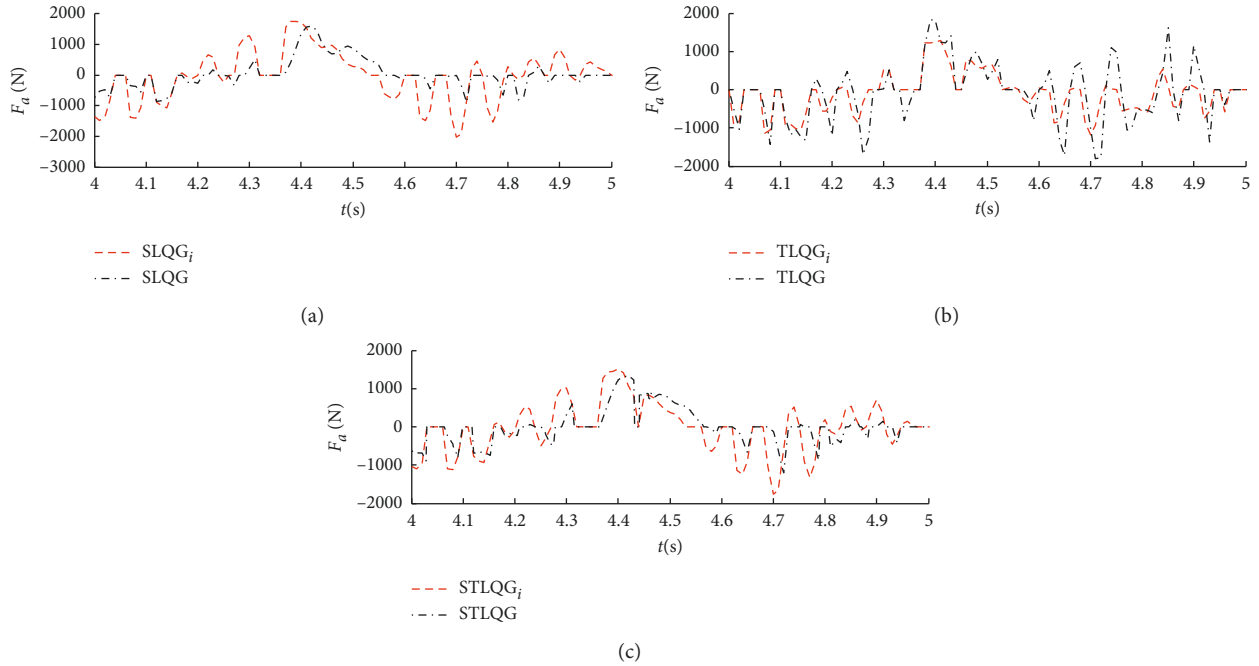

Figure 7: F_a-t curves under 25 ms time delay (partial enlargement).

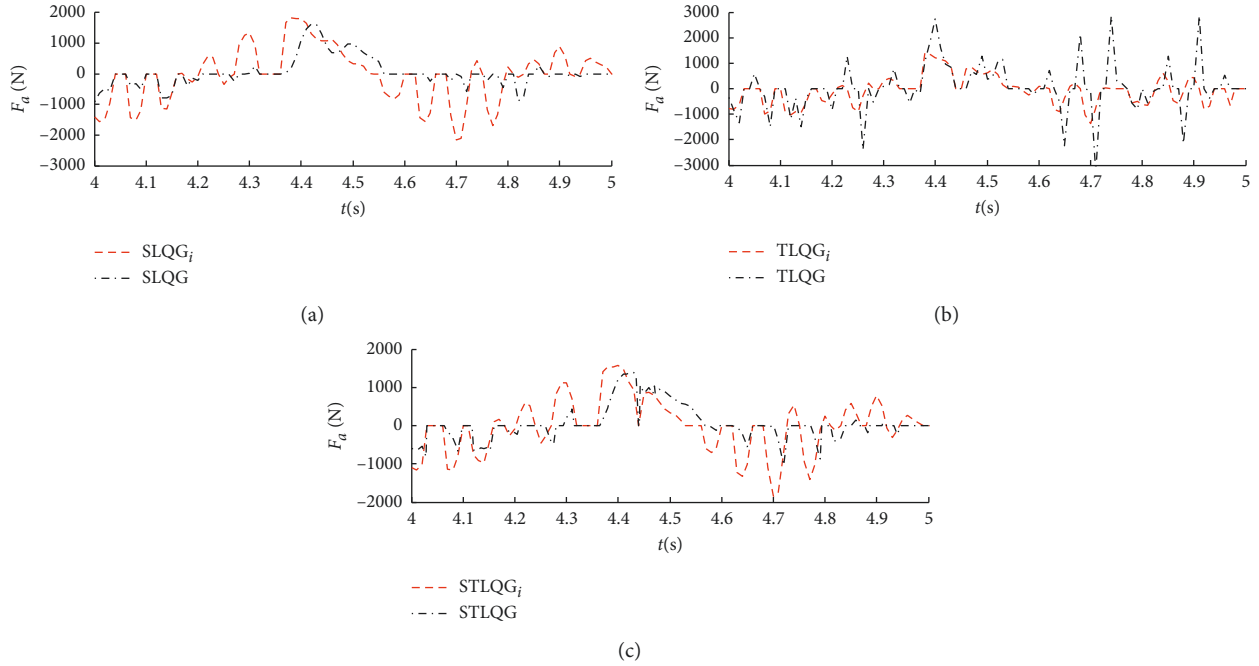

Figure 8: F_a-t curves under 30 ms time delay (partial enlargement).

following tables, RMS (a_2) stands for the root-mean-square value of a_2, RMS ($z_1 - q$) represents the root-mean-square value of $z_1 - q$, and RMS ($z_2 - z_1$) is the root-mean-square value of $z_2 - z_1$.

Table 3 illustrates that the performance deteriorates sharply when the LQG control is used. The STLQG control can reduce RMS (a_2) effectively. When time delay is 22 ms, 25 ms, 28 ms, and 30 ms, the STLQG control can, respectively, obtain 25.31%, 23.86%, 22.56%, and 22.07% reduction in RMS (a_2), compared with the Passive control. Under the four different time delays, the quadratic performance index J of the STLQG decreases 29.40%, 26.36%, 22.28%, and 20.17%, respectively, compared with the passive suspension. However, RMS ($z_1 - q$) will increase when the STLQG, SLQG, and TLQG controller are utilized. It is because that the actuator's ability to deal with high-

Table 2: Simulation results of the actual semiactive control force.

Evaluator (N)	STLQG	SLQG	TLQG
$\tau = 15$ ms			
σ (F_d)	293.7	373.8	201.9
$\tau = 20$ ms			
σ (F_d)	368.9	455.8	400.9
$\tau = 25$ ms			
σ (F_d)	415.3	513.4	530.2
$\tau = 30$ ms			
σ (F_d)	472.7	1814.6	716.9

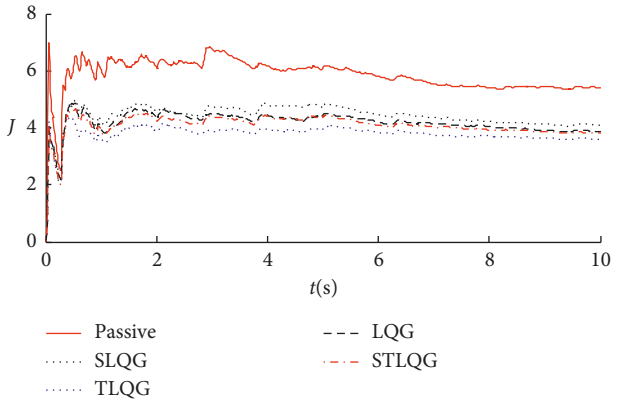

Figure 9: J-t curves under 15 ms time delay.

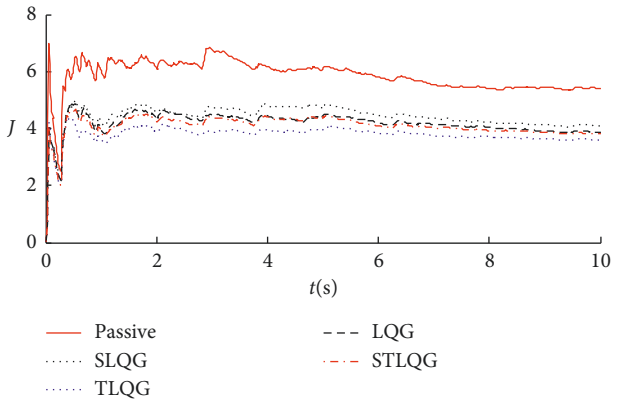

Figure 10: J-t curves under 20 ms time delay.

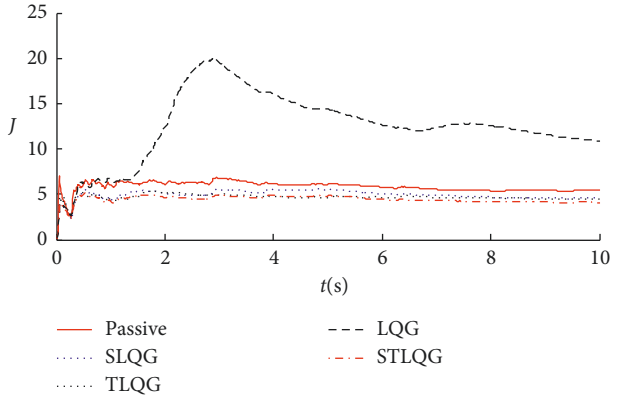

Figure 11: J-t curves under 25 ms time delay.

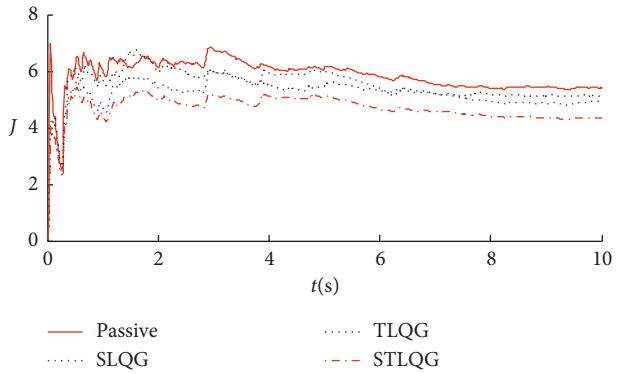

Figure 12: J-t curves under 30 ms time delay.

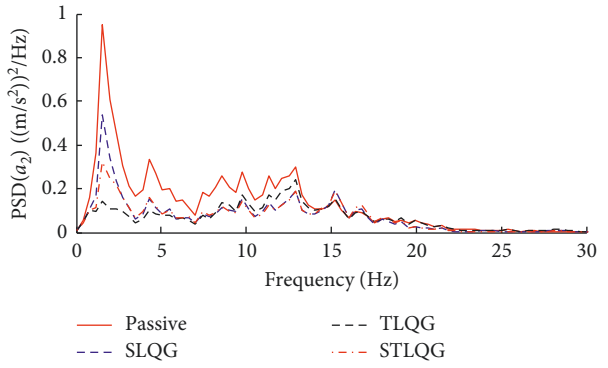

Figure 13: PSD (a_2)-frequency curves under 15 ms time delay.

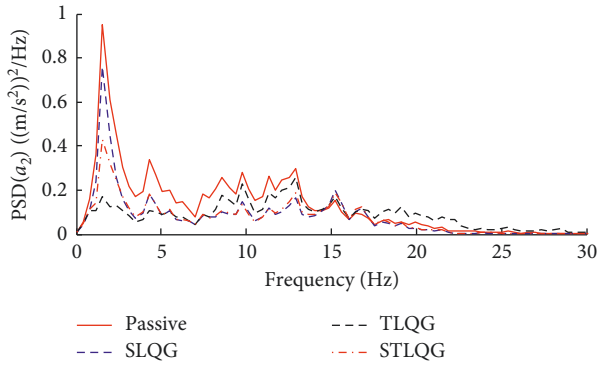

Figure 14: PSD (a_2)-frequency curves under 20 ms time delay.

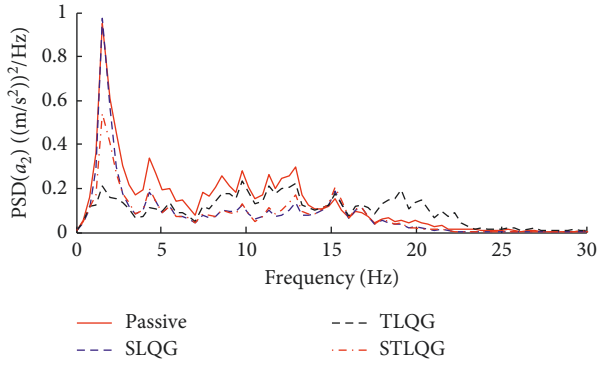

Figure 15: PSD (a_2)-frequency curves under 25 ms time delay.

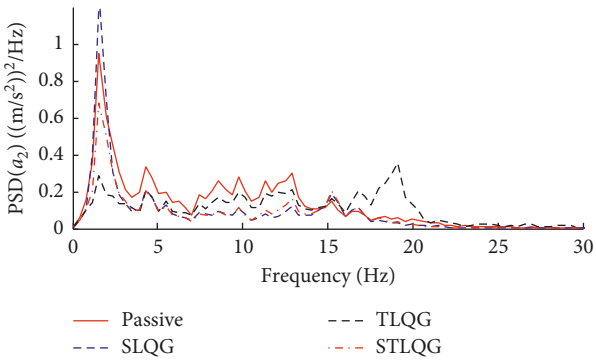

Figure 16: PSD (a_2)-frequency curves under 30 ms time delay.

Table 3: Simulation results of the passive, LQG, STLQG, SLQG, and TLQG control.

Evaluator	Passive	LQG	STLQG	SLQG	TLQG
$\tau = 15$ ms					
RMS (a_2) (m/s^2)	2.0249	1.5224	1.5124	1.5522	1.4704
RMS ($z_1 - q$) (m)	0.0040	0.0043	0.0042	0.0044	0.0039
RMS ($z_2 - z_1$) (m)	0.0107	0.0112	0.0109	0.0111	0.0112
J	5.3929	3.8067	3.8075	4.0075	3.6146
$\tau = 20$ ms					
RMS (a_2) (m/s^2)	2.0249	1.6387	1.5418	1.5994	1.6458
RMS ($z_1 - q$) (m)	0.0040	0.0050	0.0044	0.0047	0.0038
RMS ($z_2 - z_1$) (m)	0.0107	0.0115	0.0109	0.0115	0.0110
J	5.3929	4.5892	3.9712	4.3978	3.9722
$\tau = 25$ ms					
RMS (a_2) (m/s^2)	2.0249	2.1771	1.568	1.6382	1.7959
RMS ($z_1 - q$) (m)	0.0040	0.01	0.0046	0.0049	0.0039
RMS ($z_2 - z_1$) (m)	0.0107	0.014	0.0111	0.012	0.011
J	5.3929	11.3037	4.1916	4.5640	4.5349
$\tau = 30$ ms					
RMS (a_2) (m/s^2)	2.0249	91.6688	1.5781	1.6854	1.8735
RMS ($z_1 - q$) (m)	0.0040	0.67	0.0047	0.0051	0.0041
RMS ($z_2 - z_1$) (m)	0.0107	0.6793	0.0113	0.0125	0.0112
J	5.3929	34950	4.3051	4.9304	5.3069

frequency vibration is poor. For RMS ($z_2 - z_1$), no comparable change can be found.

Table 3 suggests that the time-delayed semiactive suspension with advanced technology cannot guarantee that every evaluator is superior to the passive suspension. In order to obtain better overall performance, these three evaluators should be reasonably weighed.

5. Conclusions

The paper has firstly demonstrated the application of a newly developed STLQG control scheme to compensate time delay in the time-delayed semiactive suspension. A practical case is given to reveal the advantage of the novel STLQG control. Performance comparisons show that the STLQG control can obtain better performance.

The main contributions of this research are (1) the idea and one practical method of combining Taylor series with LQG to compensate time delay are proposed and (2) the piecewise compensation using the STLQG control is newly developed in time delay compensation to overcome the disadvantages of the SLQG and TLQG controls.

Data Availability

The data used to support the findings of this study are included within the article.

Conflicts of Interest

The authors declare that they have no conflicts of interest.

Acknowledgments

This work was supported by the Innovation and Entrepreneurship Training Program for Chinese college students (Grant No 201811481014), the National Natural Science Foundation of China (Grant No 51575239), and the Key Research and Development Project of Jiangsu Province (Grant No EB2018105).

References

[1] B. Vanavil, K. K. Chaitanya, and A. S. Rao, "Improved PID controller design for unstable time delay processes based on direct synthesis method and maximum sensitivity," *International Journal of Systems Science*, vol. 46, no. 8, pp. 1349–1366, 2015.

[2] Y.-X. Wang, D.-H. Yu, and Y.-B. Kim, "Robust time-delay control for the DC-DC boost converter," *IEEE Transactions on Industrial Electronics*, vol. 61, no. 9, pp. 4829–4837, 2013.

[3] D. Ngoduy, "Linear stability of a generalized multi-anticipative car following model with time delays," *Communications in Nonlinear Science and Numerical Simulation*, vol. 22, no. 1–3, pp. 420–426, 2015.

[4] F. C. Diego Paolo, W. Claudia, and C. P. Jose Roberto, "Symmetric bifurcation analysis of synchronous states of time-delayed coupled phase-locked loop oscillators," *Communications in Nonlinear Science and Numerical Simulation*, vol. 22, no. 1–3, pp. 793–820, 2015.

[5] H. Pan, W. Sun, and H. Gao, "Robust adaptive control of nonlinear time-delay systems with saturation constraints," *IET Control Theory and Applications*, vol. 9, no. 1, pp. 103–113, 2015.

[6] Z.-Y. Liu, C. Lin, and B. Chen, "A neutral system approach to stability of singular time-delay systems," *Journal of the Franklin Institute*, vol. 351, no. 10, pp. 4939–4948, 2014.

[7] Y. Ma, L. Fu, and Y. Cao, "Robust guaranteed cost H_∞ control for singular systems with multiple time delays subject to input saturation," *Proceedings of the Institution of Mechanical Engineers, Part I: Journal of Systems and Control Engineering*, vol. 229, no. 2, pp. 92–105, 2015.

[8] G. Z. Cao, F. F. Yap, G. Chen, W. H. Li, and S. H. Yeo, "MR damper and its application for semi-active control of vehicle suspension system," *Mechatronics*, vol. 12, no. 7, pp. 963–973, 2002.

[9] C. Y. Lai and W. H. Liao, "Vibration control of a suspension system via a magnetorheological fluid damper," *Journal of Vibration and Control*, vol. 8, no. 4, pp. 527–547, 2002.

[10] L.-H. Zong, X.-L. Gong, C.-Y. Guo, and S.-H. Xuan, "Inverse neuro-fuzzy MR damper model and its application in vibration control of vehicle suspension system," *Vehicle System Dynamics*, vol. 50, no. 7, pp. 1025–1041, 2012.

[11] Y. H. Yoon, M. J. Chop, and K. H. Kim, "Development of a reverse continuous variable damper for semi-active suspension," *International Journal of Automotive Technology*, vol. 3, no. 1, pp. 27–32, 2002.

[12] H. Metered, "Application of nonparametric magnetorheological damper model in vehicle semi-active suspension system," *SAE International Journal of Passenger Cars—Mechanical Systems*, vol. 5, no. 1, pp. 715–726, 2012.

[13] D.-S. Yoon, Y.-J. Park, and S.-B. Choi, "An eddy current effect on the response time of a magnetorheological damper: analysis and experimental validation," *Mechanical Systems and Signal Processing*, vol. 127, pp. 136–158, 2019.

[14] M. F. Zhu, W. W. Chen, and H. Zhu, "Time-delay variable structure control for semi-active suspension based on magneto-rheological damper," *Journal of Mechanical Engineering*, vol. 46, no. 12, pp. 113–120, 2010.

[15] Y. Zhao, K. K. Zhou, Z. X. Li, and B. Yao, "Time lag of magnetorheological damper semi-active suspensions," *Journal of Mechanical Engineering*, vol. 45, no. 7, pp. 221–227, 2009.

[16] J. Lei, Z. Jiang, Y. L. Li, and W.-X. Li, "Active vibration control for nonlinear vehicle suspension with actuator delay via I/O feedback linearization," *International Journal of Control*, vol. 87, no. 10, pp. 2081–2096, 2014.

[17] G. I. K. Taffo and M. S. Siewe, "Parametric resonance, stability and heteroclinic bifurcation in a nonlinear oscillator with time-delay: application to a quarter-car model," *Mechanics Research Communications*, vol. 52, pp. 1–10, 2013.

[18] Y. Zhao, W. Sun, and H. Gao, "Robust control synthesis for seat suspension systems with actuator saturation and time-varying input delay," *Journal of Sound and Vibration*, vol. 329, no. 21, pp. 4335–4353, 2010.

[19] N. Janse van Rensburg, J. L. Steyn, and P. S. Els, "Time delay in a semi-active damper: modelling the bypass valve," *Journal of Terramechanics*, vol. 39, no. 1, pp. 35–45, 2002.

[20] R. Li, M. Zhou, M. Wu, and X. Tang, "Semi-active predictive control of isolated bridge based on magnetorheological elastomer bearing," *Journal of Shanghai Jiaotong University (Science)*, vol. 24, no. 1, pp. 64–70, 2019.

[21] P. Roengruen, V. Tipsuwanporn, P. Puawade, and A. Numsomran, *Smith Predictor Design by CDM for Temperature Control System*, Vol. 35, World Academy of Science, Engineering and Technology, Istanbul, Turkey, 2009.

[22] J.-L. Deltour and F. Sanfilippo, "Introduction of Smith predictor into dynamic regulation," *Journal of Irrigation and Drainage Engineering*, vol. 124, no. 1, pp. 47–52, 1998.

[23] M. Fliess, R. Marquez, and H. Mounier, "An extension of predictive control, PID regulators and Smith predictors to some linear delay systems," *International Journal of Control*, vol. 75, no. 10, pp. 728–743, 2002.

[24] M. Yu, X. M. Dong, S. B. Choi, and C. R. Liao, "Human simulated intelligent control of vehicle suspension system with MR dampers," *Journal of Sound and Vibration*, vol. 319, no. 3–5, pp. 753–767, 2009.

[25] G. Song and C. C. Xu, "Stochastic optimal preview control of active vehicle suspension with time-delay consideration," *Transactions of the Chinese Society for Agricultural Machinery*, vol. 44, pp. 1–7, 2013.

[26] A. Akbari and B. Lohmann, "Output feedback H_∞/GH_2 preview control of active vehicle suspensions: a comparison study of LQG preview," *Vehicle System Dynamics*, vol. 48, no. 12, pp. 1475–1494, 2010.

[27] Mathworks Inc., *Control System Toolbox Function LQR/LQG Design*, Mathworks Inc., Natick, MA, USA, 2009.

[28] J. L. Yao, J. Q. Zheng, and W. Y. Cai, "Sliding mode model-following control of automobile semi-active suspension system," *Transactions of the Chinese Society of Agricultural Machinery*, vol. 39, no. 4, pp. 5–8, 2008.

[29] O. J. M. Smith, "Closed control of loops with dead time," *Transactions of the Chemical Engineering Progress*, vol. 53, pp. 217–219, 1957.

[30] O. J. M. Smith, "A controller to overcome dead time," *ISA Transactions*, vol. 6, no. 2, pp. 28–33, 1959.

[31] G. Alevisakis and D. E. Seborg, "An extension of the Smith predictor method to multivariable linear systems containing time delays," *International Journal of Control*, vol. 17, no. 3, pp. 541–551, 1973.

[32] S. Chen, R. He, H. Liu, and M. Yao, "Probe into necessity of active suspension based on LQG control," *Physics Procedia*, vol. 25, pp. 932–938, 2012.